Articles in PresS. Am J Physiol Cell Physiol (July 1, 2009). doi:10.1152/ajpcell.00519.2008

Mechanisms underlying Andersen's syndrome pathology in skeletal muscle are revealed in human myotubes.

[1]Sacconi S., [2]Simkin D., [1]Arrighi N., [3]Chapon F., [4]Larroque M.M., [5]Vicart S., [6]Sternberg D., [5]Fontaine B., [2]Barhanin J., [1*]Desnuelle C. and [2*]Bendahhou S.

[1]CHU of Nice – Centre de Référence Maladies Neuromusculaires et SLA - INSERM U 638 / IFR 50, Nice, France.
[2]University of Nice Sophia Antipolis, TIANP, FRE 3093 CNRS, Parc Valrose, Nice, France.
[3]CHU of Caen, Service de Neurologie et Laboratoire de Neuropathologie, Caen, France.
[4]University of Nice Sophia Antipolis, IPMC, UMR 6097 CNRS, Sophia Antipolis, Valbonne, France.
[5]Centre de Référence des Canalopathies Musculaires, Fédération des Maladies du Système Nerveux; Université Pierre et Marie Curie, UMR S546; INSERM UMR 546, Paris, France.
[6]Biochemistry and Genetics, Hôpital Pitié-Salpêtrière, Assistance Publique, Hôpitaux de Paris, and UMR 546; Université Pierre et Marie Curie and INSERM, Paris, France.
* These authors have equal contribution

Running title: Andersen's syndrome *ex vivo*

Correspondence to Saïd Bendahhou
University of Nice Sophia Antipolis – FRE 3093 CNRS
Transport Ionique : Aspects Normaux et Pathologiques
Parc Valrose - 06560 Nice – France
Phone: (33) 492076552 Fax: (33) 492076550 Email: said.bendahhou@unice.fr
Words Count: -Abstract: 246

Abstract

Andersen's syndrome is a rare disorder that has been defined with a triad: periodic paralysis, cardiac arrhythmia, and development anomalies. Muscle weakness has been reported in two-thirds of the patients. *KCNJ2* remains the only gene linked to Andersen's syndrome; this gene encodes for the alpha subunit of the strong inward rectifier K^+ channel Kir2.1. Several studies have shown that Andersen's syndrome mutations lead to a loss of function of the potassium channel activity *in vitro*. However, *ex vivo* studies on isolated patient muscle tissue have not been reported.

We have performed muscle biopsies of controls and patients presenting with clinically and genetically defined Andersen's syndrome disorder. Myoblasts were cultured and characterized morphologically and functionally using the whole cell patch clamp technique. No morphological difference was observed between Andersen's syndrome and control myoblasts at each passage of the cell culture. Cellular proliferation and viability were quantified in parallel with direct cell counts and showed no difference between control and Andersen's syndrome patients. Moreover, our data show no significant difference in myoblast fusion index among Andersen's syndrome and control patients.

Current recordings carried out on myotubes revealed the absence of an inwardly rectifying Ba^{2+}-sensitive current in affected patient cells. One consequence of the Ik1 current loss in Andersen's syndrome myotubes is a shift of the resting membrane potential towards depolarizing potentials. Our data describe for the first time the functional consequences of Andersen's syndrome mutations *ex vivo* and provide clues to the K^+ channel pathophysiology in skeletal muscle.

Key words: skeletal muscle, Andersen's syndrome, K^+ channels

Introduction

Skeletal muscle excitability relies not only on an integrated tissue structure but also on many functional proteins such as ion channels. This has been well exemplified through ion channel-associated disorders. In the late 1960s, it was established that muscle fibers from myotonic goats had an abnormally low chloride conductance (8). The first genetic link between ion channels and skeletal muscle disorders came up in the early 1990s, through the identification of the first human Na^+ channel mutation associated with periodic paralysis (13, 22). Since then, many mutations have been identified on Ca^{2+}, Cl^-, and K^+ channels and were associated with disorders of the skeletal muscle (22-24,16,17,1,21). Non-dystrophic disorders of the skeletal muscle include mainly three different forms of periodic paralysis (hyper, hypo and normo kalaemic), paramyotonia congenita, myotonia, and Andersen's syndrome (AS). While periodic paralysis, myotonia and paramyotonia congenita patients present only with skeletal muscle dysfunctions related to cell excitability, AS patients have a more complex phenotype. In addition to periodic paralysis and cardiac arrhythmia, they exhibit bone malformations (3). Periodic paralyses have been described in two-third of AS patients, with a higher incidence of the hypokalaemic form compared to the hyper- or normo-kalaemic forms. AS has been linked to the *KCNJ2* gene that encodes for the inward rectifying Kir2.1 K^+ channel (21). This class of K^+ channels has two membrane spanning segments, a pore region and two intracellular segments. The crystal structure has been resolved for the bacterial form KirBac1.1 (18), confirming the overall topology and the tetrameric arrangement of the channel. Over 30 mutations have been identified on the *KCNJ2* gene, and their *in vitro* expression leads to a loss of channel function (21,26,2,5-7,10,9,4,11). The Kir2.1 channel can form a heterotetramer, where a mutated subunit may poison the whole protein and produce a silent channel. In addition to channel gating defects at the cell membrane, channel trafficking has also been reported as a mechanism in AS mutants (5).

AS patients present with cardiac arrhythmias that include frequent ventricular ectopy, polymorphic ventricular tachycardia, bidirectional ventricular

tachycardia, and torsades de pointes. A hallmark of AS individuals is the presence of prominent U-waves on electrocardiograms. In the heart, Kir2.1 channels produce what is known as the Ik1 current that mainly acts in the late repolarizing phase of the cardiac action potential and also in setting the cardiac myocyte resting membrane potential (20). This situation is less clear in the skeletal muscle tissue owing the prominent Cl^- conductance at rest and the structural complexity of this tissue. To date, all available data on the functional consequences of AS mutations come from *in vitro* expression of these channels either in *Xenopus* oocytes or from mammalian expression studies. In the present study, we monitor the behavior of the Ik1 current in human myoblasts from control individuals and from AS patients.

Kir2.1 channels have been shown to underlay myotube hyperpolarization, a prerequisite for myoblast fusion and differentiation (19,12). Using a Kir2.1 anti-sense RNA strategy in clonal human skeletal muscle cultures, Fischer-Lougheed and colleagues showed that silencing Kir2.1 function leads to defective myoblast fusion and inhibits myotube formation (12). These observations are interesting and may contribute to explaining the developmental anomalies in AS patients. In the present study, we address this issue using AS myoblasts with naturally occurring mutations in their native environment.

Materials and Methods

***Patients** :*

Patient A1 : A 31 years-old man, presented, since the second decade of life with episodes of painful cramps and contractures after intense exercise followed by 24-48 hours of extreme fatigue. Other trigger factors described were stress and infections. During these episodes, creatine kinase values were 2-3 fold of normal values but no myoglobinuria was noted. The frequency of these episodes increased with age from 1 per month to 1-2 per week. There was no history of tobacco, alcohol, or drug abuse; he left school at the age of 16 due to learning difficulties and is now unemployed.

His past medical history included delayed dentition, and surgical intervention for cleft palate repair. His father (patient A2) experienced the same symptoms from the age of 15 until the age of 50. The paternal grandfather died suddenly at the age of 45 with no apparent risk factors for coronary heart disease.

Patient A1 had short stature (156 cm), a distinctive craniofacial dysmorphism that included broad forehead, mild facial asymmetry, downslanting palpebral fissures, thin upper lip, long nose, dental anomalies (crowing of teeth and enamel abnormalities), and high arched palate. Neurological exam was remarkable for proximal symmetric weakness of lower limbs. The diagnosis was established because he presented an episode of hypokalaemic generalized paralysis after corticosteroid therapy for pharyngolaryngitis. Electrocardiogram revealed the presence of a prominent U wave with a normal QTc interval.

Patient A2: Father of patient A1, a 68 years-old man experienced from the age of 15 painful cramps and contractures after sustained exercise followed by 24-48 hours fatigue that made him unable to walk. No myoglobinuria was ever referred. The frequency of these episodes was 1-2 time a week when he was 25 and 35, then decreased until disappearing at the age of 50. The trigger factors he described were exercise, immobility, stress, infections, and cold. He apparently never experienced hypokalaemic periodic paralysis. He left school at the age of 13 and worked in a factory, but is now retired. He was diagnosed with type II diabetes and arterial hypertension at the age of 45. Physical examination showed short stature (150 cm), mild facial asymmetry,

downslanting palpebral fissures, dental anomalies (crowing of teeth and enamel abnormalities), and scoliosis. The neurological examination and cardiac investigations were unremarkable.

Analysis of the *KCNJ2* gene revealed a missense mutation G689A corresponding to the amino acid substitution C154Y on the Kir2.1 protein, in both patients A1 and A2.

Patient A3 : A 37 years-old caucasian man with a positive family history (mother and younger brother affected) presented, since the age of 29, episodes of hypokalaemic periodic paralysis, with a frequency of 2 to 3 episodes per year. Major triggers were exercise, rest post exercise, and stress. Apart from these episodes, he experienced episodic pain associated with sustained cramps in the lower legs, mostly in the calves, and in his hands. At the examination, he presented slight dysmorphisms that include short palpebral fissures, thin upper lips, high arched palate, mild facial asymmetry, and long nose. Electrocardiogram analysis revealed the presence of U waves. Muscle biopsy was performed on *vastus lateralis* muscle but histological and immunohistochemical examinations were normal.

The patient harbored a G1163A mutation on *KCNJ2* gene leading to the R312H amino acid substitution on the Kir2.1 protein.

Myotonia patient : A 63 year-old man who had been experiencing myotonia since childhood. The myotonia was increased by cold, hunger, fatigue and emotional upset and associated with myalgia. He also complained since the age of 45 of difficulty in climbing stairs. At the clinical and neurological examination, he displayed generalized muscle hypertrophy without any muscle weakness at rest. The creatine kinase values were normal. The electromyographic evaluation showed myotonia that was most evident in distal territories and was worsened by cold.

The disease is present in the family as an autosomal dominant trait. A mutation that corresponds to G230E amino acid substitution of the muscular chloride channel (ClC-1), that has already been described as pathogenic (14) was found in all affected members.

Cell culture set up and expansion.

Myoblasts were obtained from *vastus lateralis* muscle biopsies (dry weight ~200µg) from 3 AS patients during the diagnostic process and as *res nullus* after orthopaedic surgery from 2 matched controls. The cells were seeded as described earlier (27). The proliferation medium contained: 80% Ham's F10 (Invitrogen), 20% defined fetal bovine serum (Hyclone), antibiotics, 10 ng/mL human recombinant bFGF (R&D systems), 10^{-6} M dexamethasone (Merck). The cultures were harvested by trypsinization and expanded until they reached 80% confluence. Cell morphology was observed at each passage by inverted phase-contrast microscopy. In parallel, a phenotypic characterization was performed.

Phenotypic characterization

Myogenic cells were characterized by the presence of the surface CD56 antigen. At each passage direct labeling was performed using the phycoerythrin-coupled anti-CD56 antibody (Becton Dickinson). Non-specific labeling was evaluated using the control isotype (IgG2b, Pharmingen). Following centrifugation, the pellet was rinsed with phosphate buffered saline (PBS) and the cells were suspended under 200 µL, then analyzed by FACS (Facscalibur, Becton Dickinson) using the Cell Quest software. At least 10^4 events were analyzed. The whole cell population was visualized using a dot plot representation (FSC *vs* SSC) and the cell labeling was quantified using the density plot representation (FSC *vs* FL2).

Myoblasts proliferation studies

Populations of myoblasts at passage 5 of culture, containing over 95% CD56 positive cells were used (see above). Cells (10^4) were seeded in 12-well dishes in 1-mL proliferation medium. Each point was evaluated in triplicate. Each consecutive day, three wells were randomly selected for harvesting and counting of the cells. The medium was removed using a tip, the cell layer was washed once with pre-warmed Ca^{2+}/Mg^{2+}-free PBS and 500 µL of pre-warmed trypsin-EDTA (0.25%, Gibco) were added. Cells were incubated for 5 minutes, and suspended by several cycles of aspirations and flow reversal using a 2-mL

pipette. Their detachment and the homogeneity of the suspension were controlled by microscope inspection. 20 µL were used for cell count using a Malassez glass cytometer (all lines counted). The calculation formula was:

T = N x 1000 x dilution

T : total number of cells per mL of initial suspension. N : number of cells in the counting area of the slide. Dilution is 0.5 in the present study.

The mean of the three wells was calculated. The proliferation study generally extended over five-six days, by that time confluence was reached and formation of myotubes was observed. Doubling times were calculated as previously described (27). At the beginning and at the end of the study, CD56 phenotyping was performed by FACS in order to check if the CD56 percentage remained stable during the proliferation test.

Viability assessment

Following trypsinization and a wash with PBS, 140 µL of cell suspension was mixed with 50 µL of 0.3 mg/mL 2,3-bis(2-methoxy-4-nitro-5-sulfophenyl)-2H-tetrazolium-5-carboxanilide (XTT, Roche) for 4 h at 37°C. Absorbance was measured spectrophotometrically at 490 nm using an ELISA plate reader. An increase of number of living cells results in an increase in the overall activity of mitochondrial dehydrogenases in the sample. This increase is directly correlated to the amount of orange formazan formed, as monitored by the absorbance.

Differentiation studies.

Twenty thousand cells (CD56 purity >95 %) were seeded into 12-well plate chamber slides and allowed to proliferate for 72 hours. Differentiation was induced by replacement of the proliferation medium to the differentiation medium containing Ham's F10 (Invitrogen, 98%), 2% fetal bovine serum and antibiotics. At different time points corresponding respectively to the cell cycle withdrawal (D0), 24 hours (D1), 72 hours (D3) and 144 hours (D6) after inducing differentiation, cells were permeabilized and fixed by cold methanol (-20°C, 5 min). The cells were stained for isoforms of myosin heavy chain

(MyHC): anti-fast MyHC (Sigma), anti-slow MyHC (Sigma). Following incubation with goat anti-mouse (Ig Alexa Fluor 568), the cells were mounted under coverslips using the Vectashield Plus DAPI solution (Vector). Negative controls were obtained by substitution of the primary antibody with non immune serum. The cells were visualized using an inverted microscope equipped with fluorescence (Olympus Optical Co). Pictures were acquired using a Photometric digital camera. The number of nuclei stained with DAPI, in mononuclear cells and in multinuclear structures (myotubes from controls and AS) were determined at D3 and D6 after inducing differentiation (at least 500 myotubes were considered in 5 to 10 randomly selected fields). The fusion index was calculated using the formula:

FI = ((number of nuclei within myotube structures)/(total number of nuclei in the field) x 100).

Cell culture and Electrophysiology

Human myoblasts cultured and characterized as described above were maintained at 37 ˚C in a humidified 5 % CO_2 atmosphere in the following culture medium: 80% HAM-F10, 20% calf serum, 10 ng/mL bFGF, 1 µM dexamethasone, 2 mM glutamine, 100 U/mL penicillin, and 100 U/mL streptomycin.

Cells were differentiated using the following medium: DMEM, 10 µg/mL human insulin, 100 µg/mL pyruvate-Na, 5 µg bovine transferrin, 100 U/mL penicillin, and 100 U/mL streptomycin.

Recordings were conducted in the whole-cell configuration (15) at room temperature (~24˚C), using an EPC 10 amplifier (HEKA Electronic, Germany). The pipette solution contained (mM): 110 KCl, 5 mM NaCl, 2 $MgCl_2$, 10 EGTA, and 5 mM HEPES, pH 7.3. The bathing media was (mM): 100 N-Methyl-D-Glucamine-Cl, 5 KCl, 2 $MgCl_2$, 50 mM NaOH, 50 mM acetic acid, and 5 HEPES pH 7.3. Pipette resistance was 1.5-4 MΩ. Membrane currents were elicited by depolarizations ranging from –120 mV to +40 mV, from a holding potential of –80 mV. Only cells with series resistance less than 5 MΩ were used for analysis. Data acquisition and analysis was performed using Patchmaster and Fitmaster

(HEKA Electronic, Germany), and IgorPro (WaveMetrics Inc., OR, USA) software.

Resting membrane potential (RMP) was monitored using patch and sharp electrodes. Measurement of RMP with patch electrodes was achieved by switching the amplifier from whole cell mode to current clamp mode and by applying zero current value. RMP was also monitored with intracellular sharp electrodes filled with 3 M KCl. Borosilicate glass capillaries (GC 150 F, Clark Electromedical Instruments) were pulled with a Brown-Flamming puller (P97, Sutter Instruments Co.) and had resistances of 150-200 MΩ.

Results

Cell culture, morphology, phenotypic characterization

We have identified three AS patients and two novel mutations, C154Y and R312H, in the Kir2.1 protein. The two amino acid substitutions occur at two known sites associated with AS (10,7), and produce a loss of function when studied *in vitro*. Biopsies from *vastus lateralis* muscle were performed on each patient as well as on matched controls. No morphological difference was observed between Andersen and control myoblasts at each passage of the cell culture. The percentage of CD56-positive cells reached a plateau (above 90%) within two passages and remained elevated throughout the culture in both control and AS cell cultures.

Myoblast proliferation and viability study

Cell viability was evaluated by a colorimetric assay at each step of the cultures. The assay was based on the cleavage of the yellow tetrazolium salt XTT into an orange formazan dye by metabolically active cells. This conversion occurs only in living cells and is catalyzed by mitochondrial dehydrogenases (25). Cellular proliferation and viability were quantified through the XTT assays in parallel with the direct cell counts (data not shown). Proliferation curves reached maximal growth rates between D3 and D4, then doubling times remained stable until D5 (Figure 1). Between D4 and D5, control cells reached a doubling time of ~24h (i.e. 23.97 ± 0.75 h). At the same time, cells from the three AS patients showed similar doubling times (23.50 h, 24.67 h, and 22.17 h). The mean doubling time of AS cells was similar to controls (23.44 ± 1.25 h). Linear correlation between XTT absorbance and cell counts was confirmed showing viability rates at D4 and D5 between 80 and 95%.

Differentiation studies

It has been previously suggested that the Kir2.1 channel is involved in cell membrane hyperpolarization, which is required for myoblast fusion and differentiation. Therefore, the alteration in Kir2.1 function may result in impaired myoblast fusion and inhibition of myotube formation (12). These results

prompted us to study the *in vitro* myogenic differentiation of AS myoblasts by three different approaches. The Myoblast fusion index was calculated at four different time points after inducing differentiation, however, no statistically significant difference was detected between control and AS cell cultures (80%, 88% and 87% for AS cells, and 83% in both controls; Table 1). In addition, the average number of nuclei within the AS myotubes was comparable to the controls (C, 4.1 ± 3 and AS, 4.2 ± 2.8 for D3; C, 12 ± 1.2 and AS, 12.1 ± 1 for D6). There was also, no difference in myotube morphology nor in fast or slow myosin heavy chain expression immunostaining (Figure 2)

Ionic currents in control human muscle cells

Human myoblasts obtained from biopsied patients undergoing orthopaedic surgery were cultured in 35-mm dishes in normal culture medium. Current recordings were performed 24 h later on isolated cells to prevent cell coupling. In these conditions, only small inward and outward currents were recorded (Figure 3A). The outward current is likely to be carried out by Kv2.1 channels as has already been described in H9c2 myoblasts (28). After ten days of differentiation (under insulin with low or no serum), the outward currents became larger and additional currents were observed including fast inactivating currents, likely to represent the voltage-gated Na^+ currents, and small sustained inwardly rectifying currents that we suspect to underlay Ik1 currents (Figure 3B,3C,3E). The fast inactivating currents were indeed completely abolished after application of 500 nM tetrodotoxin (TTX) to the bathing medium without altering other ionic current activities (Figure 3C). When combining 500 µM $BaCl_2$ and 500 nM TTX in the bathing medium, the inward rectifier currents were also blocked (Figure 3D). Representative current-voltage relationships were drawn from the upper traces, at the end of the test pulse. The current amplitude of the curves represents the inward currents and outward currents. These data not only show an increase in the outward currents after cell differentiation, but more importantly to this study, an increase in an inwardly rectifying current (Figure 3G) that is blocked by low Ba^{2+} concentrations (Figure 3H).

Ionic currents in Andersen's syndrome muscle cells

Skeletal muscle biopsies from three AS patients were used to culture myoblasts as described above. Currents elicited by successive depolarizations of undifferentiated AS muscle cells show a pattern similar to that seen with undifferentiated cells from healthy individuals: small outward currents (Figure 4A, 4B). After differentiation, similarly to muscle cells from healthy individuals, the outward currents became larger and fast inactivating and TTX-sensitive currents develop in most of the cells recorded. However, the inward rectifying currents were missing in the vast majority of the cells monitored (Figure 4C, 4D).

Current density in human muscle cells

Overall, three kinds of currents were recorded in our experimental conditions after cell differentiation. Cell capacitance was monitored for each cell and current density was calculated as the ratio of the current amplitude to the cell capacitance. For the inward rectifying currents, the current amplitude was measured at -120 mV at the end of a 500-ms test pulse. The current densities were averaged for both normal controls as well as for AS patients. The current density (pA/pF) at -120 mV was significantly lower for AS patients than that for control individuals (Figure 5A, 5B; $p < 0.0001$). Maximum peak current was also monitored at -20 mV and current density was calculated for each value. Our data show that AS muscle cells have significantly higher Na^+ channel density than healthy individuals ($p < 0.01$) (Figure 5C). However, current density at +40 mV was only slightly but still significantly higher for AS patients than controls ($p < 0.05$) (Figure 5D).

Andersen's syndrome myotubes are depolarized at rest

After recording ionic currents in voltage clamp mode, cells were switched to current clamp mode and rest membrane potential was measured from all differentiated muscle cells. Our data show that the rest membrane potential significantly shifted towards depolarizing potentials for AS patients compared to control individuals (-51.68 ± 1.39 mV, n= 38 for controls; -46.70 ± 0.55 mV, n=

154 for AS; $p < 0.001$) (Figure 6A). All rest membrane potential values monitored for controls as well as for AS were more depolarized than that of native muscle tissue, this is probably due to a combination of low K^+ concentrations used in our intracellular medium, and a heterogeneous cell population (19). To further confirm that the AS resting membrane potential is more depolarized than in controls, an intracellular sharp electrode technique was used (-54.7 ± 0.4 mV, n= 121 for controls; -43.2 ± 0.8 mV, n= 83 for AS; $p < 0.0001$) (Figure 6B).

Ionic currents in a myotonia patient

All parameters monitored in the muscle cells of control and AS patients were compared to those of the patient with myotonia congenita, with the G230E amino acid substitution on the skeletal muscle ClC-1 chloride channel. Whole cell current recordings from muscle cells of the myotonia patient showed a pattern similar to that of healthy individuals, *i.e.* large Na^+ and outward currents, and the presence of an inwardly rectifying current (Figure 7A). Current densities at -120 mV were not significantly different between those recorded in cells obtained from the myotonia patient and those obtained from the healthy individuals ($p = 0.582$), however, they were significantly higher than those recorded in AS myotubes ($p < 0.0001$) (Figure 7B). At -20 mV, the current density in myotonia myotubes was not significantly different from that of healthy myotubes ($p = 0.0526$), but significantly lower than that of AS myotubes ($p < 0.0001$) (Figure 7C). The current density recorded at the end of the +40-mV test pulse in myotonia myotubes was not significantly different from that of healthy ($p = 0.231$) as well as AS myotubes ($p = 0.355$) (Figure 7D). Finally, the rest membrane potential was investigated and showed that myotonia and AS myotubes were similarly and significantly depolarized compared to myotubes from healthy individuals ($p < 0.001$) (Figure 7E).

Discussion

After the identification of the *KCNJ2* gene as the genetic entity associated with AS, functional studies have shown, in heterologous expression systems, that the disorder is associated with a loss of function of the K^+ channel Kir2.1 protein. The skeletal muscle manifestations in AS patients were characterized by muscle weakness leading to either one of the three forms of periodic paralyses, without myotonia. Although, the hypokalaemic form was the most frequently described, since it was reported in two-thirds of the AS patients.

To better understand the skeletal muscle pathophysiology, muscle biopsies were performed on two patients with the C154Y amino acid substitution and one patient carrying the R312H mutation in the Kir2.1 protein. The three patients have typical clinical manifestations reminiscent of AS: periodic paralysis, development anomalies, and cardiac arrhythmia. We have previously described AS mutations occurring at the same sites (C154F and R312C) (7,10). The mutated channels produced a loss of function when expressed *in vitro*. However, their behavior as well as that of all other AS mutations has not been monitored *ex vivo*. Using biopsied muscle from control individuals and from 3 AS patients, we were able to describe cell proliferation, differentiation, fusion, and expression in these myoblasts.

We first characterized phenotypically the behavior of the cultured myoblasts. We made sure that our cell population was largely made of muscle cells, using myoblast markers and showed that the percentage of myoblasts in the culture reached at least 98%. Cell proliferation, fusion and differentiation were monitored for both controls and AS myoblasts during 6 passages. By contrast to previous studies, we did not detect any difference between myoblasts from healthy individuals and those from AS patients. Indeed, it has been suggested that the Kir2.1 channel is involved in cell membrane hyperpolarization, which is required for myoblast fusion and differentiation (12). It has also been suggested that the alteration in Kir2.1 function would result in impaired myoblast fusion and inhibition of myotube formation. These conclusions were based on anti-sense RNA assays for Kir2.1 in clonal cultures. Our observations are based on naturally occurring mutations in a human tissue without any

441 modification of the cellular environment. Over-expressing anti-sense RNA into
442 myoblasts may have interfered not only with Kir2.1 expression, but with other
443 cellular pathways required for proliferation and fusion. Additionally, using anti-
444 sense RNA for Kir2.1 may have completely knocked out the Ik1 current, which
445 may not be the case for a K^+ channel with a tetrameric structure in a native
446 tissue. In fact, in an autosomal dominant disorder, and with a mutated subunit
447 that poisons whole channel function, there is a $1/16^{th}$ chance of a combination
448 that would result in a WT-like channel, which, would lead to the expression of a
449 fraction of the Ik1 current in the myoblasts. This may be sufficient to ensure
450 myotube formation. Alternatively, other compensatory mechanisms may have
451 taken place in AS human myoblasts, but may have been prevented in intrusive
452 systems such as anti-sense RNA. Interestingly, Kir2.1 channel knockout mice
453 die shortly after birth, due to a cleft in the secondary palate, but no muscle
454 abnormalities have been reported (29,30).
455 Further characterization of control and AS myoblasts involves the ionic activity
456 at the cell membrane. Both cell types express the same level of the outward
457 current when undifferentiated. Interestingly, this current resembles the outward
458 current that has already been described in H9c2 myoblasts, a clonal cell line
459 derived from embryonic rat ventricle and represents an *in vitro* model for cardiac
460 and skeletal muscle myocytes. Kv2.1 channels were shown to underlay this
461 current (28). However, the ionic current composition and magnitude were not
462 identical after cell differentiation. Cells from healthy control individuals express a
463 large outward current, an inward TTX-sensitive current, and an inwardly
464 rectifying Ba^{2+}-sensitive current. Compared to control cells, AS differentiated
465 myoblasts express all currents except the inwardly rectifying Ba^{2+}-sensitive
466 current that was recorded in the control cells. We hence conclude that the
467 inwardly rectifying Ba^{2+}-sensitive current is the signature of Kir2.1 K^+ channel
468 activity in human skeletal muscle myotubes. Our data also show that this is the
469 first evidence that AS-associated Kir2.1 mutations lead to a loss of channel
470 function in human skeletal muscle cells. The first consequence of the absence
471 of the Ik1 current in human myoblasts is a significant depolarization of the rest
472 membrane potential. This depolarization is similar to that seen in myotubes from

a myotonia patient with a *ClCN1* mutation. However, AS patients do not exhibit myotonia, but only periodic paralysis. Even though myotonia and AS myotubes have a common functional defect, the functional consequences are opposite on the skeletal muscle pathophysiology, suggesting that the two ion channels do not play the same role in the skeletal muscle structure. While chloride channels have buffering properties to maintain or bring back membrane potential to its initial value, potassium channels tend to set the cell rest membrane potential. This is a major difference between the two classes of ion channels but it does not explain the mechanism by which AS mutations lead to muscle paralysis. Our system relies on native human cells, and clearly shows the loss of Kir2.1 function in AS myotubes, however it does not reconstitute the complex skeletal muscle architecture that may be needed to further understand the pathogenic mechanism of AS mutations.

Acknowledgments

We thank the patients for their kind participation. We thank G. Romey for his kind help with sharp electrode technique. This work was supported by the Centre National de la Recherche Scientifique (CNRS), and by a grant from the Association Française contre les Myopathies (AFM) to S.B. and by a student fellowship to D.S. The authors acknowledge the collaboration of Résocanaux, a clinical and research network funded by Agence National de la Recherche (ANR) and GIS Maladies Rares.

References

1. **Abbott GW, Butler MH, Bendahhou S, Dalakas MC, Ptáček LJ, Goldstein SA.** MiRP2 forms potassium channels in skeletal muscle with Kv3.4 and is associated with periodic paralysis. *Cell* 104 **:** 217-231, 2001.
2. **Andelfinger G, Tapper AR, Welch RC, Vanoye CG, George AL, Benson DW.** *KCNJ2* mutation results in Andersen syndrome with sex-specific cardiac and skeletal muscle phenotypes. *Am J Hum Genet* 71 : 663-668, 2002.
3. **Andersen ED, Krasilnikoff PA, Overvad H.** Intermittent muscular weakness, extrasystoles, and multiple developmental anomalies. A new syndrome? *Acta Paediatr Scand* 60 : 559-564, 1971.
4. **Ballester LY, Benson DW, Wong B, Law lH, Mathews KD, Vanoye CG, George AL.** Trafficking-competent and trafficking-defective *KCNJ2* mutations in Andersen syndrome. *Hum Mutat* 27 **:** 388, 2006.
5. **Bendahhou S, Donaldson MR, Plaster NM, Tristani-Firouzi M, Fu YH, Ptáček LJ.** Defective potassium channel Kir2.1 trafficking underlies Andersen-Tawil syndrome. *J Biol Chem* 278 : 51779-51785, 2003.
6. **Bendahhou S, Fournier E, Gallet S, Menard D, Larroque MM, Barhanin J.** Corticosteroid-exacerbated symptoms in an Andersen's syndrome kindred. *Hum Mol Genet* 16 : 900-906, 2007.
7. **Bendahhou S, Fournier E, Sternberg D, Bassez G, Furby A, Sereni C, Donaldson MR, Larroque MM, Fontaine B, Barhanin J.** *In vivo* and *in vitro* functional characterization of Andersen's syndrome mutations. *J Physiol (Lond)* 565 : 731-741, 2005.
8. **Bryant SH.** Cable properties of external intercostal muscle fibres from myotonic and nonmyotonic goats. *J Physiol (Lond)* 204 **:** 539-550, 1969.
9. **Davies NP, Imbrici P, Fialho D, Herd C, Bilsland LG, Weber A, Mueller R, Hilton-Jones D, Ealing J, Boothman BR, Giunti P, Parsons LM, Thomas M, Manzur AY, Jurkat-Rott K, Lehmann-Horn F, Chinnery PF, Rose M, Kullmann DM, Hanna MG.** Andersen-Tawil syndrome: new potassium channel mutations and possible phenotypic variation. *Neurology* 65 **:** 1083-1089, 2005.
10. **Donaldson MR, Jensen JL, Tristani-Firouzi M, Tawil R, Bendahhou S, Suarez WA, Cobo AM, Poza JJ, Behr E, Wagstaff J, Szepetowski P, Pereira S,**

Mozaffar T, Escolar DM, Fu YH, Ptáček LJ. PIP2 binding residues of Kir2.1 are common targets of mutations causing Andersen syndrome. *Neurology* 60 **:** 1811-1816, 2003.

11. **Eckhardt LL, Farley AL, Rodriguez E, Ruwaldt K, Hammill D, Tester DJ, Ackerman MJ , Makielski JC.** *KCNJ2* mutations in arrhythmia patients referred for LQT testing: A mutation T305A with novel effect on rectification properties. *Heart Rhythm* 4 : 323-329, 2007.
12. **Fischer-Lougheed J, Liu JH, Espinos E, Mordasini D, Bader CR, Belin D, Bernheim L.** Human myoblast fusion requires expression of functional inward rectifier Kir2.1 channels. *J Cell Biol* 153 **:** 677-686, 2001.
13. **Fontaine B, Khurana TS, Hoffman EP, Bruns GA, Haines JL, Trofatter JA, Hanson MP, Rich J, McFarlane H, Yasek DM, Romano D, Gusella JF, Brown RH.** Hyperkalemic periodic paralysis and the adult muscle sodium channel alpha-subunit gene. *Science* 250 **:** 1000-1002, 1990.
14. **George AL, Crackower MA, Abdalla JA, Hudson AJ, Ebers GC.** Molecular basis of Thomsen's disease (autosomal dominant myotonia congenita). *Nature Genet* 3**,** 305-310, 1993.
15. **Hamill OP, Marty A, Neher E, Sakmann B, Sigworth FJ.** Improved patch-clamp techniques for high-resolution current recording from cells and cell-free membrane patches. *Pflugers Arch* 391 **:** 85-100, 1981.
16. **Jurkat-Rott K, Lehmann-horn F, Elbaz A, Heine R, Gregg RG, Hogan K, Powers PA, Lapie P, Valesantos JE, Weissenbach J, Fontaine B.** A calcium channel mutation causing hypokalemic periodic paralysis. *Hum Mol Genet* 3 **:** 1415-1419, 1994.
17. **Koch MC, Steinmeyer K, Lorenz C, Ricker K, Wolf F, Otto M, Zoll B, Lehmann-Horn F, Grzeschik KH, Jentsch TJ.** The skeletal muscle chloride channel in dominant and recessive human myotonia. *Science* 257 **:** 797-800, 1992.
18. **Kuo A, Gulbis JM, Antcliff JF, Rahman T, Lowe ED, Zimmer J, Cuthbertson J, Ashcroft FM, Ezaki T, Doyle DA.** Crystal structure of the potassium channel KirBac1.1 in the closed state. *Science* 300 **:** 1922-1926, 2003.
19. **Liu JH, Bijlenga P, Fischer-Lougheed J, Occhiodoro T, Kaelin A, Bader CR, Bernheim L.** Role of an inward rectifier K^+ current and of hyperpolarization in

562 human myoblast fusion. *J Physiol (Lond)* 510 **:** 467-476, 1998.
563 20. **Lopatin AN, Nichols CG.** Inward rectifiers in the heart: an update on I(K1). *J Mol*
564 *Cell Cardiol* 33 **:** 625-638, 2001.
565 21. **Plaster NM, Tawil R, Tristani-Firouzi M, Canun S, Bendahhou S, Tsunoda A,**
566 **Donaldson MR, Iannaccone ST, Brunt E, Barohn R, Clark J, Deymeer F,**
567 **George AL, Jr., Fish FA, Hahn A, Nitu A, Ozdemir C, Serdaroglu P, Subramony**
568 **SH, Wolfe G, Fu YH, Ptáček LJ.** Mutations in Kir2.1 cause the developmental and
569 episodic electrical phenotypes of Andersen's syndrome. *Cell* 105 **:** 511-519, 2001.
570 22. **Ptáček LJ, George AL, Griggs RC, Tawil R, Kallen RG, Barchi RL, Robertson**
571 **M, Leppert MF.** Identification of a mutation in the gene causing hyperkalemic
572 periodic paralysis. *Cell* 67 **:** 1021-1027, 1991.
573 23. **Ptáček LJ, Tawil R, Griggs RC, Engel AG, Layzer RB, Kwiecinski H, McManis**
574 **PG, Santiago L, Moore M, Fouad G, Bradleyc P, Leppert MF.** Dihydropyridine
575 receptor mutations cause hypokalemic periodic paralysis. *Cell* 77 **:** 863-868, 1994.
576 24. **Ptáček LJ, Trimmer JS, Agnew WS, Roberts JW, Petajan JH, Leppert M.**
577 Paramyotonia congenita and hyperkalemic periodic paralysis map to the same
578 sodium-channel gene *locus*. *Am J Hum Genet* 49 **:** 851-854, 1991.
579 25. **Roehm NW, Rodgers GH, Hatfield SM, Glasebrook AL**. An improved
580 colorimetric assay for cell proliferation and viability utilizing the tetrazolium salt XTT.
581 *J Immunol Methods* 142 **:** 257-265, 1991.
582 26. **Tristani-Firouzi M, Jensen JL, Donaldson MR, Sansone V, Meola G, Hahn A,**
583 **Bendahhou S, Kwiecinski H, Fidzianska A, Plaster N, Fu YH, Ptáček LJ, Tawil**
584 **R.** Functional and clinical characterization of *KCNJ2* mutations associated with
585 LQT7 (Andersen syndrome). *J Clin Invest* 110 **:** 381-388, 2002.
586 27. **Vilquin JT, Marolleau JP, Sacconi S, Garcin I, Lacassagne MN, Robert I,**
587 **Ternaux B, Bouazza B, Larghero J, Desnuelle C**. Normal growth and
588 regenerating ability of myoblasts from unaffected muscles of facioscapulohumeral
589 muscular dystrophy patients. *Gene Ther* 12 **:** 1651-1662, 2005.
590 28. **Wang W, Hino N, Yamasaki H, Aoki T, Ochi R**. KV2.1 K^+ channels underlie
591 major voltage-gated K^+ outward current in H9c2 myoblasts. *Jap J Physiol* 52 **:** 507-
592 514, 2002.
593 29. **Zaritsky JJ, Eckman DM, Wellman GC, Nelson MT, Schwarz TL**. Targeted

disruption of Kir2.1 and Kir2.2 genes reveals the essential role of the inwardly rectifying K(+) current in K(+)-mediated vasodilation. *Circ Res* 87 **:** 160-166, 2000.

30. **Zaritsky JJ, Redell JB, Tempel BL, Schwarz TL**. The consequences of disrupting cardiac inwardly rectifying K(+) current (I(K1)) as revealed by the targeted deletion of the murine Kir2.1 and Kir2.2 genes. *J Physiol* 533 **:** 697-710, 2001.

Legend to Figures

Figure 1: Andersen's syndrome skeletal muscle cells have normal proliferation

Each day, two independent samples of Andersen's syndrome (A1, A2, A3) or control cells were trypsinized and incubated with XTT for 4 hours at 37°C. Spectrophotometrical absorbance was measured at 490 nm. The data were presented as the mean ± SEM.

Figure 2: Myogenic differentiation on Andersen syndrome and control myoblasts.

Contrast phase images (A, B) at day 6 (D6) as well as immunostaining for fast (C,D) and slow (E,F) myosin heavy chain isoforms did not show any difference in myotube morphology and myosin expression between controls (A,C,E) and Andersen syndrome myoblasts (B,D,F). DAPI staining was used for nuclei (C-F).

Figure 3: Ionic currents in healthy human myoblasts

Ionic currents and current-voltage relationships from undifferentiated (A,F) or differentiated (B,C,D,E,G,H) myoblasts were recorded in the whole cell configuration. The currents shown in A, B, C, and D are obtained from 4 different cells. (E) is only an enhancement of panel C showing the inwardly rectifying current that can be elicited with the first 5 depolarizations (-120 mV to -40 mV).

Tetrodotoxin (TTX) 500 nM and $BaCl_2$ 500 µM were added to the bathing medium where indicated. (G) Current-voltage relationship from a differentiated myoblast. (H) Current-voltage relationship from a differentiated myoblast treated with 500 nM TTX and 500 µM $BaCl_2$. Block with TTX revealed no difference in the sustained currents. Current values were obtained at the end of the 500-ms test pulse from -120 mV to +40 mV, in 20-mV increment.

Figure 4: Lack of Ik1 currents in Andersen's syndrome myotubes

Ionic currents, and related current-voltage relationships, from undifferentiated (A,B) or differentiated (C,D) myoblasts from Andersen's syndrome patients were recorded in the whole cell configuration. Current values were obtained at the end of the 500-ms test pulse as described for control cells.
Note the absence of the inwardly rectifying Ba^{2+}-sensitive current in Andersen's syndrome myotubes.

Figure 5: Current density in myotubes from healthy and from Andersen's syndrome patients.
(A) Steady-state currents were monitored at the end of the 500-ms test pulse at -120 mV for 4 healthy individuals (C1, C2, C3, and C4) and for 3 Andersen's syndrome patients (A1, A1, and A3). (B) Current densities were determined and averaged for controls and for Andersen's syndrome patients. (C) Current densities were obtained from the peak current at -20 mV test pulse for the TTX-sensitive component. (D) Current densities are shown for the outward current component and measured at +40 mV at the end of a 500-ms test pulse. Values are Mean ± SEM. The number of cells recorded is shown above the bar graphs.

Figure 6: Resting membrane potential is depolarized in Andersen's syndrome myotubes
Resting membrane potential was determined by switching cells from voltage clamp to current clamp configuration after rupturing into the cell (A), or by using intracellular sharp electrode technique (B). Membrane potential at rest is depolarized in myotubes from Andersen's syndrome patients compared to those obtained from healthy controls. Values are Mean ± SEM. Significantly different (* P< 0.05, **, P<0,001).

Figure 7: Andersen's syndrome and myotonia myotubes are similarly depolarized
(A) Whole cell current traces from myotonia myotubes. Currents were elicited by -120 mV to +40 mV test pulses in 20-mV increments. Current densities were determined in myotonia myotubes, at -120 mV (B), at -20 mV (C), or at + 40 mV

(D) and were compared to AS and control cells. (E) Resting membrane potential was monitored for myotonia myotubes as described above. Values are Mean ± SEM.

Table 1: Fusion index of myoblasts remains intact in Andersen's syndrome cells Myoblast fusion index for two healthy individuals (C1, C2) and for three Andersen's syndrome patients (A1, A2, A3), at day 0 (D0) and at day 6 (D6) of differentiation. Values are Mean ± SEM for 3 experiments

Figure 1

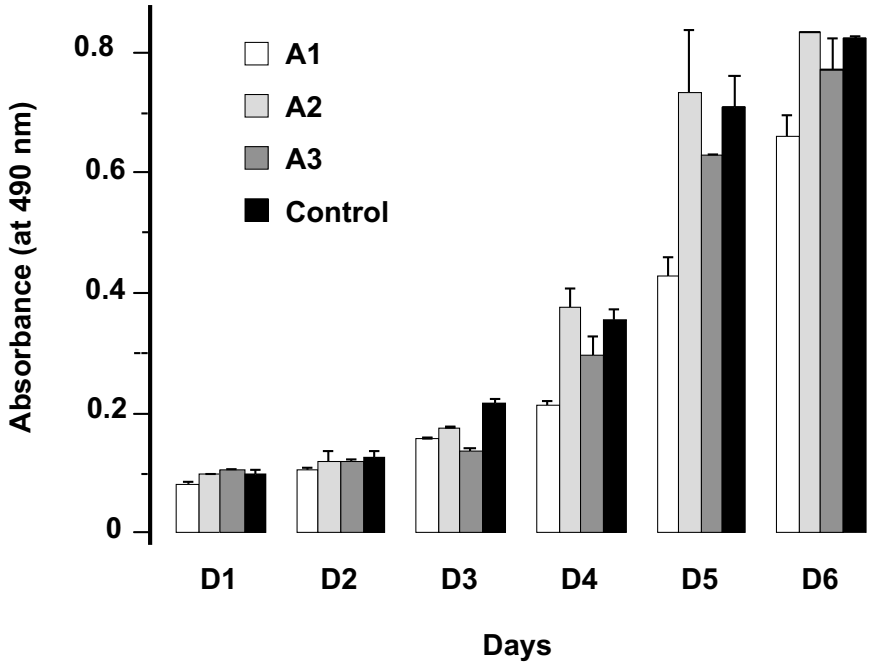
Absorbance (at 490 nm)
0.8
0.6
0.4
0.2
0
A1
A2
A3
Control
D1
D2
D3
D4
D5
D6
Days

Figure 2

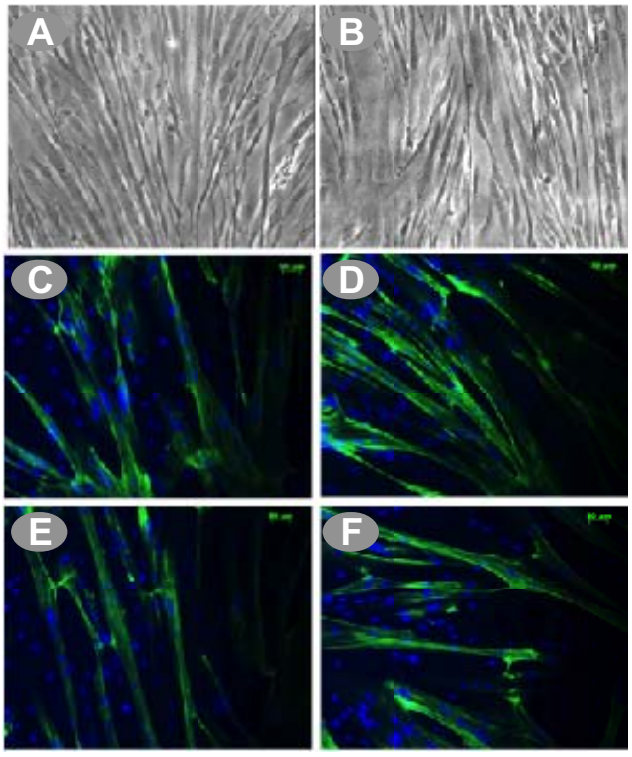

Figure 3

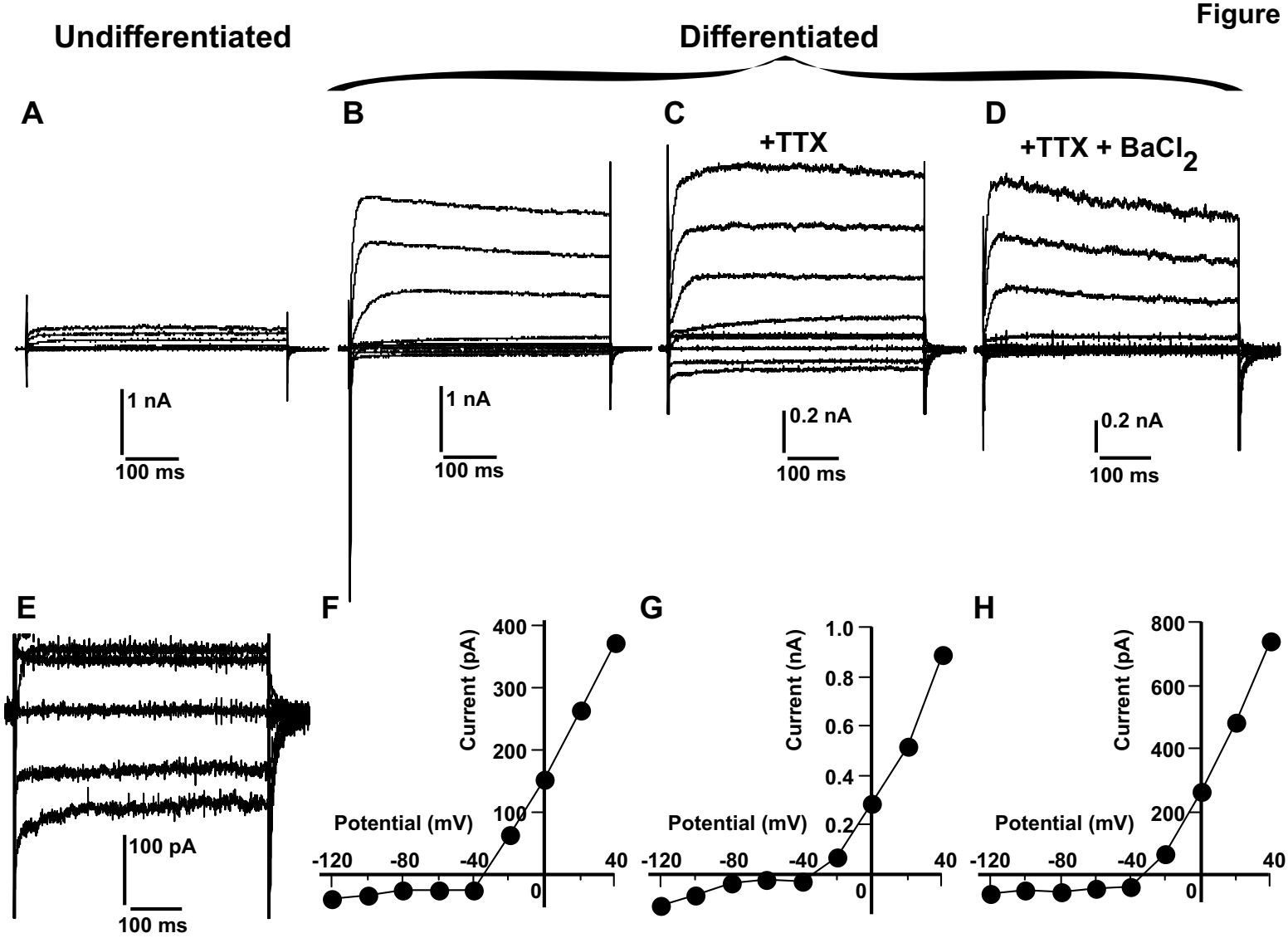
Undifferentiated
Differentiated
A
B
C
D
+TTX
+TTX + BaCl2
1 nA
100 ms
1 nA
100 ms
0.2 nA
100 ms
0.2 nA
100 ms
E
F
G
H
100 pA
100 ms
Current (pA)
Potential (mV)
400
300
200
100
-120
-80
-40
40
0
Current (nA)
1.0
0.8
0.6
0.4
0.2
Current (pA)
800
600
400
200

Figure 4

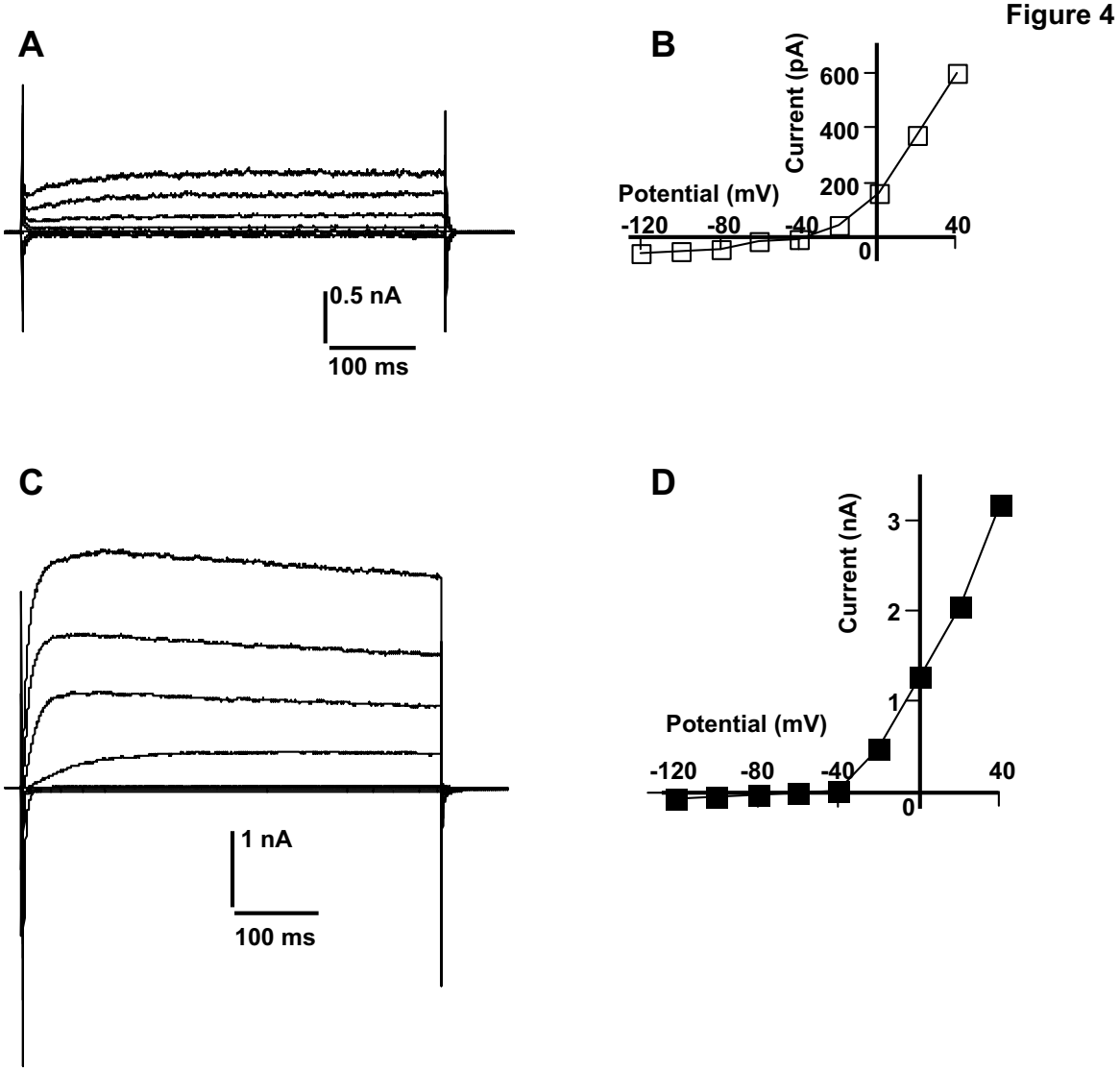
A
0.5 nA
100 ms
B
Current (pA)
600
400
200
Potential (mV)
-120
-80
-40
0
40
C
1 nA
100 ms
D
Current (nA)
3
2
1
Potential (mV)
-120
-80
-40
0
40

Figure 5

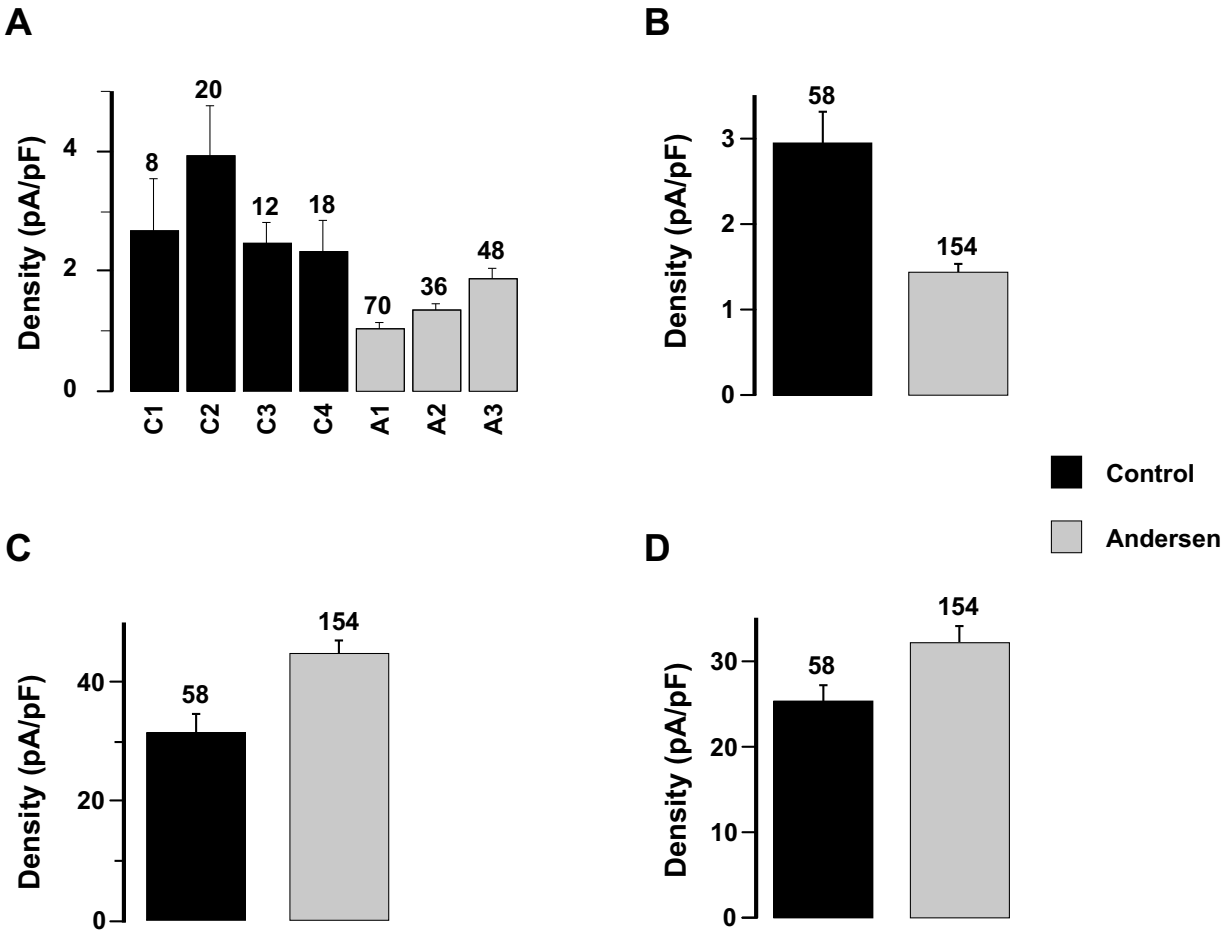
A
Density (pA/pF)
0
2
4
8
20
12
18
70
36
48
C1
C2
C3
C4
A1
A2
A3
B
Density (pA/pF)
0
1
2
3
58
154
Control
Andersen
C
Density (pA/pF)
0
20
40
58
154
D
Density (pA/pF)
0
10
20
30
58
154

Figure 6

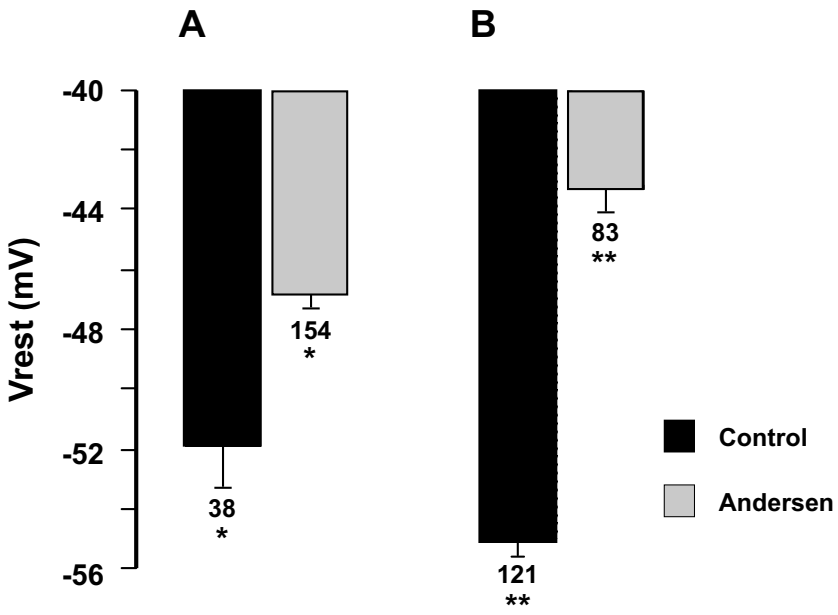

Figure 7

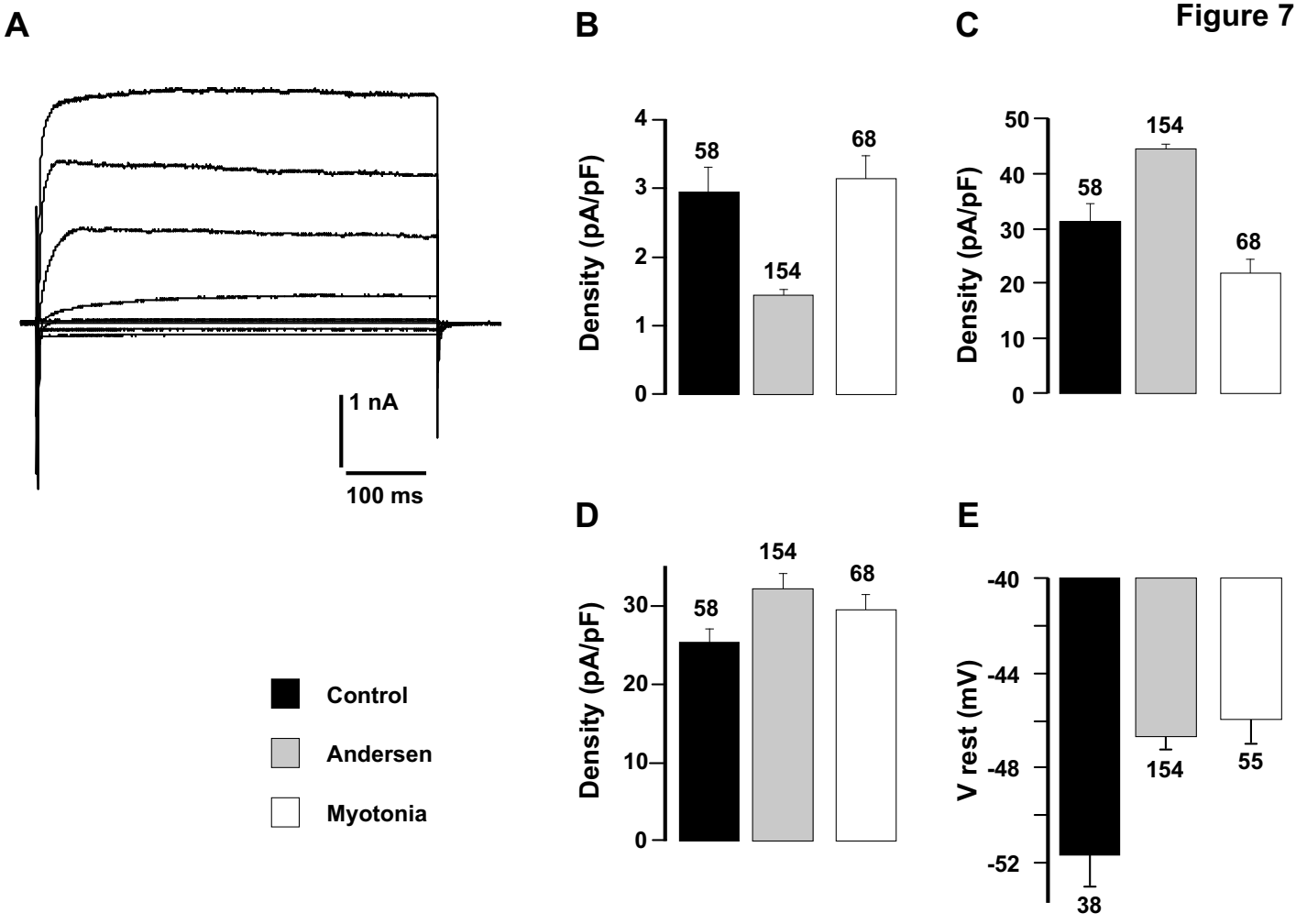
A
1 nA
100 ms
Control
Andersen
Myotonia
B
Density (pA/pF)
0
1
2
3
4
58
154
68
C
Density (pA/pF)
0
10
20
30
40
50
58
154
68
D
Density (pA/pF)
0
10
20
30
58
154
68
E
V rest (mV)
-40
-44
-48
-52
38
154
55

Table 1

Patients	D0 FI %	D1 FI %	D3 FI %	D6 FI %
C1	2.5 ± 0.5	11.2 ± 2.3	39.2 ± 4.5	83.3 ± 1.5
C2	1.0 ± 0.1	10.5 ± 3.1	41.3 ± 3.4	83.6 ± 5.5
A1	1.7 ± 0.7	10.9 ± 3.4	40.1 ± 3.3	80.6 ± 1.1
A2	2.1 ± 0.7	11.1 ± 1.9	38.5 ± 5.5	88.3 ± 1.1
A3	1.0 ± 0.0	12.0 ± 0.8	41.1 ± 3.3	87.3 ± 2.1

C: Control; A: Andersen petient; D: Day; FI: Fusion Index